

1 **Unravelling the evolutionary history and future prospects of endemic**
2 **species restricted to former glacial refugia**

3 Orly Razgour¹, Irene Salicini², Carlos Ibáñez², Ettore Randi^{3,4}, Javier Juste²

4 ¹ Division of Biological and Environmental Sciences, School of Natural Sciences, University of
5 Stirling, Stirling FK9 4LA, Scotland, UK

6 ² Estación Biológica de Doñana (CSIC), Avda Americo Vesputio s/n 41092 Seville, Spain

7 ³ Laboratorio di Genetica, Istituto Superiore per la Protezione e Ricerca Ambientale, Ozzano Emilia,
8 Bologna, Italy

9 ⁴ Department 18/ Section of Environmental Engineering, Aalborg University, Sohngårdsholmsvej 57,
10 9000, Aalborg, Denmark

11

12 **Keywords:** Approximate Bayesian Computation, Bats, Climate Change, Species Distribution

13 Modelling, *Myotis escaleraei*, Phylogeography

14 **Corresponding Author:**

15 Orly Razgour

16 Division of Biological and Environmental Sciences, School of Natural Sciences, University of

17 Stirling, Stirling FK9 4LA, Scotland, UK

18 Fax: +44 1786 467843; Email: Orly.Razgour@gmail.com

19

20 **Running Title:** Climate change and restricted endemic species

21 **Abstract**

22 The contemporary distribution and genetic composition of biodiversity bear a signature of
23 species' evolutionary histories and the effects of past climatic oscillations. For many
24 European species, the Mediterranean peninsulas acted as glacial refugia and the source of
25 range re-colonisation, and as a result they contain disproportionately high levels of diversity.
26 As these areas are particularly threatened by future climate change, it is important to
27 understand how past climatic changes affected their biodiversity. We use an integrated
28 approach, combining markers with different evolutionary rates, and combining phylogenetic
29 analysis with Approximate Bayesian Computation and species distribution modelling across
30 temporal scales. We relate phylogeographic processes to patterns of genetic variation in
31 *Myotis escalerai*, a recently confirmed bat species endemic to the Iberian Peninsula. We
32 found a distinct population structure at the mitochondrial level with a strong geographic
33 signature, indicating lineage divergence into separate glacial refugia within the Iberian
34 refugium. However, the microsatellite dataset suggests higher levels of gene flow resulting in
35 more limited structure at recent time frames. The evolutionary history of *M. escalerai* was
36 shaped by the combined effects of climatic oscillations and changes in forest cover and
37 composition, while its future is threatened by climatically-induced range contractions and the
38 role of ecological barriers in restricting its distribution. This study warns that Mediterranean
39 peninsulas, which provided refuge for European biodiversity during past glaciation events,
40 may become a trap for limited dispersal and ecologically-restricted endemic species under
41 future climate change, resulting in loss of entire lineages that evolved under past climatic
42 isolation mechanisms.

43 **Introduction**

44 The contemporary distribution and genetic composition of biodiversity bear a signature of
45 species' evolutionary histories. Quaternary climatic oscillations, in the form of recurring
46 glacial-interglacial cycles, resulted in substantial range shifts, population extinctions and
47 lineage divergences (Hewitt 2000), though effects varied with latitude, topography (Hewitt
48 2004) and individual species' adaptations and environmental tolerances (Stewart *et al.* 2010).

49 With the advent of molecular tools, the study of the distribution of biodiversity was extended
50 to include genetic relationships between individuals and the influence of historical processes
51 on the geographic distribution of genetic lineages (Avice 2000). Phylogeography has provided
52 the framework to determine the causal links between geography, climate change, ecological
53 interactions and the evolution of taxa (Hickerson *et al.* 2010). Its integration with ecological
54 niche modelling has helped elucidate the processes and mechanisms shaping genetic variation
55 and the evolutionary trajectories of species and populations (Alvarado-Serrano & Knowles
56 2014). Understanding the phylogeographic structure of species, and the mechanisms that
57 sustain it, is integral to conserving their full genetic diversity and to managing evolutionary
58 significant units within species according to their differing regional vulnerabilities (Schmitt
59 2007). Moreover, understanding species' responses to past events may help us better predict
60 the potential consequences of future climatic changes (Hofreiter & Stewart 2009).

61 During Pleistocene glacial periods, much of northern and central Europe was covered by ice
62 sheets and permafrost. The Mediterranean peninsulas of Iberia, Italy and the Balkans acted as
63 glacial refugia for many European species and as the source of rapid northern range
64 colonisation during interglacial, warmer climatic periods. Cycles of contraction-expansion
65 into and out of glacial refugia resulted in a genetic signature of southern richness with deep

66 divergence between refugial populations versus northern impoverishment and genetic
67 homogeneity (Hewitt 2004). Stable areas that persisted across glaciation cycles harbour
68 particularly high levels of species richness (Araújo *et al.* 2008) and unique genetic diversity
69 (Hampe & Petit 2005), and as a result are of high evolutionary importance (Stewart *et al.*
70 2010). However these hotspots of genetic diversity are particularly threatened by future
71 climate change (EEA 2012; Razgour *et al.* 2013), and therefore it is important to understand
72 how past climatic changes affected their biodiversity.

73 The Iberian Peninsula has a rich and well-studied biogeographic history. Its complex
74 topography and geographic position between the Mediterranean and North Atlantic create
75 distinct bioclimatic regions with ecologically and genetically divergent taxa (Gomez & Lunt
76 2007). Yet this great environmental heterogeneity, combined with relative climatic stability
77 and long-term lineage persistence and divergence without large geographic displacement,
78 makes it more difficult to interpret the genetic population structure and evolutionary history
79 of species within Iberia (Hewitt 2001; Rodriguez-Sanchez *et al.* 2010). The Iberian Peninsula
80 played an important role in the evolutionary history of European bats. Phylogeographic
81 studies of widely-distributed European bat species show that although Iberia was an important
82 glacial refugium for many species it did not necessarily contribute to post-glacial range re-
83 colonisation because lineages remained isolated inside the peninsula by the Pyrenees
84 mountain range (e.g. *Barbastella barbastellus*, Rebelo *et al.* 2012; and *Rhinolophus*
85 *hipposideros*, Dool *et al.* 2013). However for other bat species, the Iberian refugium was the
86 main source of range re-colonisation, while the Alps formed a stronger barrier to range
87 expansion from other Mediterranean refugia (e.g. *Myotis myotis*, Ruedi & Castella 2003).

88 Here we set to unravel the effect of Quaternary climatic oscillations on the evolutionary
89 history of *Myotis escalerai*, a bat species endemic to the Iberian Peninsula (defined here as the
90 area including Spain, Portugal, the Balearic Islands, Andorra and the French Pyrenees), and to
91 determine factors that limit its distribution and how it will be affected by future climate
92 change. *M. escalerai* is part of the *Myotis nattereri* cryptic species complex (*M. nattereri*
93 *sensu stricto*, *M. escalerai*, *M. spA*, and *M. spB*; Salicini *et al.* 2011) that has only recently
94 been genetically confirmed as a separated species (Ibáñez *et al.* 2006). Unlike other bat
95 species, the entire evolutionary history of *M. escalerai* took place within Iberia (Salicini *et al.*
96 2013), and therefore both its present genetic population structure and future survival are
97 closely linked to climate change processes within the Iberian Peninsula. We use an integrated
98 approach, combining markers with different evolutionary rates, and combining phylogenetic
99 analysis with Approximate Bayesian Computation (ABC) model-based inference and species
100 distribution modelling across temporal scales, to relate phylogeographic processes to
101 contemporary and future patterns of genetic variation.

102 **Methods**

103 **Sample collection**

104 Genetic samples, in the form of 3mm wing biopsies were collected from *M. escalerai* bats
105 captured in 16 colonies, located mostly in underground sites (caves), distributed across the
106 Iberian Peninsula and the Balearic island of Mallorca (Table S1, Figure 1a).

107 **Laboratory procedures**

108 Genomic DNA was extracted from all samples following the methods described in Salicini *et al.* (2013). We sequenced 750 bp of the mitochondrial DNA (mtDNA) *Cytochrome b* (*Cyt b*)
109 gene, using the primers Molcit-F (Ibáñez *et al.* 2006) and Molcit-R (Salicini *et al.* 2011). PCR
110 conditions and sequencing information are outlined in Salicini *et al.* (2013). Sequences were
111 aligned and edited using Sequencher 4.5 (Gene Codes Corp, MI, USA), and collapsed into
112 unique haplotypes with Dambe v5.2.31 (Xia & Xie 2001).

114 Samples were genotyped for 10 microsatellite loci previously published for the genus (A13,
115 D9, D15, E24, F19, G25, H29, A24, H23: Castella & Ruedi 2000; and b22: Kerth *et al.* 2002).
116 The forward primer of each locus pair was labelled fluorescently with HEX or 6-FAM
117 (Applied Biosystems). Microsatellites were combined into single or double PCR sets.
118 Each PCR mix contained 0.3µl primer sets at 10µM, 1µl of PCR Buffer 10X, 0.3µl dNTPs,
119 0.05µl TAQ and 1µl of DNA, adding H₂O up to 10µl total volume. When needed, 0.8 µl of
120 Bovine Serum Albumin was added. PCR amplification was performed using ABI Veriti
121 thermal cycler (Applied Biosystems, USA). We used the following PCR program: initial
122 denaturation at 95°C for 5min, followed by 30-40 cycles of 95°C for 30s, annealing
123 temperature from 55°C to 60°C, depending on the primers, for 45s and 72°C for 45s, followed
124 by a final extension at 72°C for 10 min. PCR products were sequenced using ABI 3130 48-
125 well DNA Sequencer. Allele sizes were assigned using the GeneMapper software (Applied
126 Biosystems, USA).

127 Observed and expected heterozygosity and estimated null allele frequencies were calculated
128 using CERVUS v3.0.3 (Kalinowski *et al.* 2007) and Micro-Checker (Van Oosterhout *et al.*
129 2004). Tests for departures from Hardy-Weinberg equilibrium and assessment of linkage

130 disequilibrium were performed in GENEPOP v4.0.10 (Raymond & Rousset 1995; Rousset
131 2008). Loci that were out of Hardy-Weinberg equilibrium and with a high frequency of null
132 alleles in several populations were removed from the analysis.

133 **Genetic data analysis**

134 *Mitochondrial dataset*

135 In addition to the samples from the 16 studied colonies, the mtDNA analysis also included *M.*
136 *escalerai* *Cyt b* sequences downloaded from Genbank that belonged to samples from the
137 French Pyrenees (FJ460363 – Evin *et al.* 2009; JF412390 and JF412391 – Puechmaille *et al.*
138 2012) and 107 *M. escalerai* sequences from individuals captured across the Iberian Peninsula
139 to better characterise the range of the species, including 21 individuals from around the
140 Pyrenees (Navarra, Huesca, Lleida and Girona) and 18 individuals from adjacent areas (La
141 Rioja, Zaragoza, Teruel and Tarragona) (Table S2; Figure 1a). We used jModelTest v2.1.6
142 (Darriba *et al.* 2012) to select the Hasegawa-Kishino-Yano (HKY) mtDNA substitution
143 model with gamma-distributed rate variation based on the Bayesian Information Criterion
144 (BIC) values. Bayesian phylogenetic trees were constructed in MrBayes v3.2.1 (Ronquist &
145 Huelsenbeck 2003), using two *Myotis spA* sequences as outgroup to root the tree. We ran
146 5×10^7 generations with four chains, sampled every 500th generation, and two simultaneous
147 runs, discarding the first 25% of trees generated as burn-in. Trees and posterior probabilities
148 were visualised with Figtree v1.3.1 (<http://tree.bio.ed.ac.uk/software/figtree/>).

149 Parsimony haplotype network was constructed with NETWORK (v4.610, Fluxus
150 Technology), employing the median-joining network algorithm and the Greedy FHP distance
151 calculation method. Nucleotide polymorphism, haplotype diversity, genetic divergence and

152 differentiation between populations were calculated in DnaSP v5.10 (Librado & Rozas 2009),
153 with 10000 permutations to obtain probability values.

154 *Microsatellite dataset*

155 Analysis of microsatellite genetic diversity, including allele frequencies, number of private
156 alleles, allelic richness, heterozygosity, gene diversity and population differentiation (F_{st}),
157 was carried out at the colony level with GenAlEx v6.4 (Peakall & Smouse 2006) and Fstat
158 v2.9.3.2 (Goudet 1995) controlling for differences in sample sizes. To test for levels of
159 relatedness among individuals, we used the Triadic Maximum Likelihood estimator (TrioML;
160 Wang 2007) implemented in Coancestry (Wang 2011) because this measure allows for
161 inbreeding and accounts for genotyping errors in the data.

162 Population structure in the microsatellite dataset was inferred using individual-based Bayesian
163 assignment tests implemented in STRUCTURE v2.3.3 (Pritchard *et al.* 2000). Number of
164 tested genetic clusters (K) ranged from 1 to 15. We performed ten independent runs for each
165 K, using the general admixture model with correlated allele frequencies and 10^6 Markov
166 Chain Monte Carlo (MCMC) generations following a burn-in phase of 5×10^5 generations.
167 The number of distinct clusters was determined using STRUCTURE HARVESTER (Earl &
168 Von Holdt 2012) based on the number of clusters at which the mean log-likelihood peaked
169 and where variation among runs was minimal (Figure S1). Cluster assignment was visualised
170 with DISTRUCT (Rosenberg 2004).

171 Because the presence of closely related individuals (in particular full siblings) can bias the
172 number of clusters identified in the STRUCTURE analysis (Rodriguez-Ramilo & Wang
173 2012), we first ran assignment tests with the whole dataset and then re-ran the analysis
174 removing individuals with TrioML values >0.5 . This threshold was selected because below

175 this value most of the pairwise estimations were among individuals from geographically
176 distant colonies (58% for TrioML =0.5, versus 2% for TrioML >0.5).

177 **Species Distribution Modelling Procedures**

178 We used Species Distribution Models (SDMs) to generate phylogeographic hypotheses for
179 testing with ABC inference, to identify environmentally stable areas where the species
180 persisted overtime, to determine the most important environmental variables limiting the
181 distribution of *M. escalerae* and to predict future changes to distribution (Alvarado-Serrano &
182 Knowles 2014). We predicted the potential distribution of suitable conditions for *M. escalerae*
183 under present, past (LGM ~21,000 years before present, and the Last Interglacial period [LIG]
184 ~130,000 ybp) and future (2070) climatic conditions. Study area extent was set as the Iberian
185 Peninsula, the Balearic Islands and France up to latitude 49.5 N and longitude 6.5 E. This
186 extent enabled the inclusion of potentially suitable areas beyond the species' currently know
187 distribution, while limiting problems associated with selecting pseudo-absences at large
188 distances from known location records (VanDerWal *et al.* 2009). Model resolution was ~1km
189 (30 arc seconds).

190 Models were generated with Maxent v3.3.3 (Phillips *et al.* 2006) using 182 location records,
191 including one location record from the French Pyrenees taken from Evin *et al.* (2009). As the
192 whole of Iberia has been sampled extensively for this species, our dataset is not likely to
193 suffer from sampling bias. All location records outside the south of Iberia were genetically
194 confirmed because of potential range overlap with cryptic congeners of the *M. nattereri*
195 species complex. We used the Average Nearest Neighbor tool in ArcGIS v10.2 (ESRI) to
196 remove duplicate and clustered location records in order to minimise spatial autocorrelation
197 between location records.

198 We ran two types of models, climatic-topographic models (climate model) for all time
199 periods, and a full model that included also habitat variables for the present only. Climatic
200 and topographic layers were downloaded from WorldClim (<http://www.worldclim.org>),
201 geological layers from One Geology (<http://www.onegeology.org/>, reclassified into 18 broad
202 categories) or USF Geoportal Data Depository (Karst Regions of the World,
203 <http://gisdata.rc.usf.edu/>, Hollingsworth *et al.* 2008). Habitat variables were obtained from the
204 European Space Agency (GlobCover 2009, http://due.esrin.esa.int/page_globcover.php) for
205 land cover (reclassified into 10 categories), European Environment Agency (Corine Land
206 Cover 2006, <http://www.eea.europa.eu/>) for woodland variables (woodland type and distance
207 to woodlands), and Hansen *et al.* (2013) for percent tree canopy cover. Multicollinearity
208 among environmental variables was tested with ENMtools v1.3 (Warren *et al.* 2010),
209 removing highly correlated variables (correlation coefficients ≥ 0.8) and variables that did not
210 contribute to the SDMs. The following layers were included in the final models: maximum
211 temperature of warmest month (BIO5), minimum temperature of the coldest month (BIO6),
212 average temperature of the driest quarter (BIO9), temperature seasonality (BIO4), annual
213 rainfall (BIO12), rainfall seasonality (BIO15), rainfall in warmest quarter (BIO18), slope,
214 altitude, distance to karsts (maternity colonies are known to form in caves; Ibáñez *et al.*
215 2006), land cover, distance to woodlands and percent tree cover.

216 Models were projected into the past using the CCSM and MIRC0 General Circulation
217 Models (GCMs) for the LGM and one LIG model. Future models for 2070 were generated
218 using three European GCMs (HadGEM2_ES, IPSL-CM5A-LR and MPI-ESM-LR), and the
219 IPCC5 +8.5 W/m² Representative Concentration Pathways (IPCC 2013), representing the
220 ‘worst case’ scenario.

221 Our modelling procedures followed recommendations in Merow *et al.* (2013). We compared
222 several models with different variables and parameter combinations (regularization values,
223 number of features included) in ENMTools, and selected the best models based on Akaike
224 Information Criterion (AIC) scores. The final full and climate models included all features
225 with a regularization value of 1, 10,000 background points and 1500 iterations. When
226 comparing models we used the raw output, but when running the final models we used the
227 cumulative output. Projected output maps generated by the different LGM or future GCMs
228 were multiplied to produce a single map per time period. In order to determine differences in
229 the extent of areas with high relative occurrence probability over time we converted model
230 outputs into binary maps using the thresholding method that maximises the sum of sensitivity
231 and specificity (Liu *et al.* 2013). Range changes were calculated for the Iberian Peninsula
232 alone (including the Pyrenees). Maps were processed in ArcGIS v10.2 (ESRI).

233 Model predictive ability was tested with five-fold cross validation and compared based on the
234 Area Under the Curve (AUC) of the Receiver Operator Characteristics. To determine whether
235 our models performed significantly better than random, we tested if our models' training and
236 test AUC scores fell outside the 95% Confidence Intervals of the distribution of the AUC
237 scores of 100 null models (Raes & ter Steege 2007), randomly generated in ENMTools with
238 the altitude layer.

239 **ABC Framework**

240 The evolutionary history of *M. escalerai* was reconstructed using the ABC approach
241 implemented in DIYABC v2.0.4 (Cornuet *et al.* 2014) to identify source populations and
242 patterns of colonisation. Phylogeographic hypotheses were generated based on paleo-SDM
243 predictions. We first ran a full analysis (Analysis 1), which included all colonies, divided into

244 three geographical groups (Western, Southern and North-Central-Eastern). The full analysis
245 aimed to identify the source population, LGM refugial populations and patterns of post-LGM
246 range recolonisation. Next we ran separate ABC analyses for the geographically separated
247 Western (Analysis 2) and Eastern (Analysis 3) groups to identify the representative putative
248 source colonies of each group in relation to predicted climatic suitability during the LGM.
249 Finally, in Analysis 4, we assessed the demographic history of the Western and Eastern
250 groups, comparing scenarios of post-LGM population expansion versus pre/post-LGM
251 population declines (Figure S8). Scenarios compared in each analysis and their specific
252 demographic parameters are outlined in Supplementary Materials.

253 ABC analyses were carried out with the combined microsatellite and mtDNA datasets as well
254 as on each dataset separately. The separate mtDNA analysis also included the 107 individual
255 samples and the two French sequences. The remaining analyses only included samples from
256 the 16 colonies. We generated 10^6 simulations for each scenario tested in each analysis. The
257 posterior probability of scenarios was estimated using a weighted polychotomous logistic
258 regression. We checked model performance and empirically evaluated the power of the model
259 to discriminate among scenarios (confidence in scenario choice) by simulating pseudo-
260 observed datasets with the different scenarios and calculating false allocation rates (type1 and
261 2 errors, Cornuet *et al.* 2010).

262 **Results**

263 **MtDNA dataset**

264 We identified 50 unique Cyt *b* haplotypes (20 from the 16 colonies). The haplotype network
265 divided the haplotypes into three separate haplo-groups: Western, Southern and North-

266 Central-Eastern. Western haplotypes were separated from the remaining haplotypes by >19
267 mutational steps. Most southern haplotypes grouped together and were separated by >8
268 mutational steps from the North-Central-Eastern haplotypes. However one haplotype from the
269 south-eastern colony Granada grouped with the North-Central-Eastern haplotypes, while most
270 of the samples from the southern colony of Sevilla grouped with the Western haplo-group.
271 Samples from the French Pyrenees belonged to the common Eastern haplotype (CasGiIB), as
272 did most samples from around the Pyrenees. However some unique haplotypes were
273 identified in the Pyrenees, all of which were separated by one mutational step from either the
274 common Eastern (CasGiIB) or North-Central (LROurSeg) haplotypes, depending on their
275 geographical location (eastern and central versus western Pyrenees) (Figure 1c, Table S1-2).

276 The Bayesian phylogenetic tree showed maximum posterior probability support for the split
277 of *M. escalerai* into two principal lineages, the Western (South-West clade in Salicini *et al.*
278 2013) and Southern clade, and the remaining haplotypes, which mainly constituted of North-
279 Central-Eastern haplotypes. The Western and Southern clades were further divided (posterior
280 probability=0.85) into the Western and Southern lineages (Figure 1b).

281 Mitochondrial haplotype diversity was highest in the North-Central-Eastern group, even after
282 accounting for differences in sample size (32 haplotypes, 0.16 per sample), but nucleotide
283 diversity was highest in the Southern group ($\pi=0.02$; Table S3). Among the colonies, Cádiz
284 and Illes Balears had the highest haplotype diversity, while Granada, Alacant and Sevilla the
285 highest nucleotide diversity (Table 1). Overall genetic differentiation at the mtDNA level
286 between the Western, North-Central-Eastern and Southern geographic groups was significant
287 ($\chi^2_{90}=678.5$, $P<0.001$; overall $\theta_{ST}=0.73$), with particularly high levels of differentiation
288 between the Western and North-Central-Eastern groups ($\theta_{ST}=0.93$; Table S4).

289 **Microsatellite data**

290 Of the ten microsatellite loci, one marker (H29) was removed due to high frequency of null
291 alleles. After removing this marker, all colonies, but Huelva, were overall in Hardy-Weinberg
292 equilibrium. None of the markers were in linkage disequilibrium and all were in Hardy-
293 Weinberg equilibrium in at least 13 out of the 16 colonies. The dataset, excluding H29,
294 contained a total of 103 alleles, with an average of 11.44 ± 5.5 alleles per locus (range 4–21),
295 and 10 private alleles.

296 Genetic diversity (adjusted for sample size) in terms of allelic richness, heterozygosity, gene
297 diversity and number of private alleles, was highest in Granada (southern Iberia) followed by
298 Cáceres (western Iberia), and was lowest in Girona (eastern Iberia) and Illes Balears (Table
299 1). Levels of relatedness were particularly high within the Girona and Illes Balears colonies
300 (mean TrioML= 0.44 ± 0.1 and 0.25 ± 0.2 , respectively), whereby a third of the pair-wise
301 relatedness values between individuals within the Girona colony were > 0.5 . Levels of
302 population differentiation were highest between Girona and all other colonies and Illes
303 Balears and all other colonies, even after the removal of close relatives. Particularly low
304 levels of differentiation were found between Cáceres and most southern and western colonies
305 and among the southern colonies (Table S5).

306 Individual-based Bayesian assignment tests detected genetic population structure in *M.*
307 *escalerai*. Individuals were best divided into four genetic clusters (\ln probability (K) = -7730
308 ± 5 ; Figure S1), despite some level of admixture in most colonies. The most north-eastern
309 colony, Girona, formed a separate cluster; however this cluster disappeared once close
310 relatives (TrioML > 0.5) were removed from the analysis. Individuals whose haplotypes
311 belonged to the mtDNA North-Central-Eastern clade tended to be assigned to different

312 clusters from individuals from the mtDNA Western clade, with the exception of individuals
313 from the most north-western colony (Ourense). However, most individuals whose haplotypes
314 belonged to the mtDNA Southern clade showed high levels of admixture between clusters,
315 and only an East to West geographic gradient was evident at the nuclear microsatellite level
316 (Figure 2).

317 **Species Distribution Modelling across temporal scales**

318 All SDMs had high predictive ability, did not overfit presence data (full model: AUC=0.89
319 $AUC_{\text{crossvalidation}}=0.80 \pm 0.04$; climatic model: AUC=0.87, $AUC_{\text{crossvalidation}}=0.79 \pm 0.03$) and had
320 significantly higher predictive ability than the null models (mean AUC=0.64 ± 0.004 [95%
321 Confidence Intervals], range: 0.57-0.67). The best fit model in terms of AIC scores had a
322 regularization value of 1. The main eco-geographical variable contributing to both the
323 climatic and full models was slope. Other important variables contributing to the climatic
324 model were annual rainfall (BIO12), temperature seasonality (BIO4), rainfall seasonality
325 (BIO15) and average temperature of the dry quarter (BIO9), while the habitat variable percent
326 tree cover and the land cover type conifer woodlands were important in the full model
327 (Figures S2-3). Both models show high concordance on predictions for areas occupied by the
328 16 colonies, though the full model offers a finer resolution, which results in more fragmented
329 habitat suitability in the north-west. All colonies, except for two western colonies (Nabão and
330 Ourense), are currently located in areas predicted to have a high relative occurrence
331 probability for *M. escalerai*, though both are still within 5 km distance of suitable areas
332 (Figure 3a-b; Figure S4).

333 Paleo-SDMs predicted a substantial decrease in the extent of suitable conditions for *M.*
334 *escalerai* in Iberia during the LGM compared with present conditions (percent of area above

335 suitability threshold for present: 34%, for LGM: 8.4%). Suitable climatic conditions during
336 the LGM were restricted to isolated areas in the central-west, south and east of Iberia and in
337 south-eastern France, while the Central Plateaus, Western Pyrenees and the north and west
338 coasts were climatically unsuitable. As a result, in the Western Group, only the most central
339 colony Cáceres and the northern colony Entrimio were located in climatically suitable areas
340 (Figure 3c-d). Model predictions were affected by variables outside their training range
341 around the Pyrenees, north-west Iberian coast and northern France (Figure S6). The extent of
342 suitable conditions was also low during the LIG (17%), but suitable areas were restricted to
343 the north Atlantic coast, western Iberia (Portugal) and the southern tip near the Strait of
344 Gibraltar (Figure S5).

345 Future SDMs predicted a reduction in range suitability for *M. escalerai* in Iberia by 2070 (to
346 18.1%) with most of the south and interior of Iberia predicted to become climatically
347 unsuitable. However, the northern Atlantic coast, Pyrenees and north-western France are
348 predicted to gain suitable areas (Figure 3e-f). This will result in the majority of colonies and
349 the entire southern lineage being located in climatically unsuitable areas by 2070. However,
350 these predictions should be considered with caution because temperature variables were
351 outside their training range across most of the Peninsula (Figure S7).

352 **ABC inference of demographic/evolutionary history**

353 Model-based inference pointed to the western group being the source population of *M.*
354 *escalerai*, and to the presence of two separate refugia in the Iberian Peninsula during the
355 LGM, one in the West and one in the North-Central-East. The Southern population diverged
356 from the Western population after the end of the LGM, and later was admixed with gene flow

357 from the North-Central-East population (Scenario 1.1, posterior probability=0.93; type 1
358 error=0.03, type 2=0.02; Figure 4a; Table S6).

359 The Western Group analysis identified Cáceres as the representative source population of the
360 Western *M. escalerai* group, from which all other colonies split after the LGM, beginning
361 with the most south-western colony (Amarela) and ending with the adjacent central colony
362 (Nabão) (Scenario 2.1, posterior probability=0.99; type1 error=0.02, type2 error=0.02; Figure
363 4b; Table S7). Similarly, Castellón was the representative source population in the best
364 supported model for the Eastern Group and all other Eastern colonies split directly from this
365 population post-LGM, with the oldest split being between Castellón and Girona (Scenario 3.1,
366 posterior probability=0.83; type 1=0.05, type 2=0.03; Figure 4b; Table S8). In both analyses,
367 population split dates were estimated to have occurred between the early and mid-Holocene.

368 Demographic history modelling indicates that the Western group's effective population size
369 has increased more than 10-fold after the end of the LGM, while the Eastern population size
370 remained stable, though currently both groups have similar estimated effective population
371 sizes (Scenario 4.3, posterior probability=1.0, type 1=0.016, type 2=0.01; Figure S8; Table
372 S9). The timing of the western population expansion corresponds with the estimated time of
373 colonisation of the south-western colonies, and therefore may reflect population expansion to
374 areas south of the LGM refugia.

375 The same full model scenario (Scenario 1.1) was supported by the microsatellite-only dataset
376 (posterior probability=0.99, type 1=0.05, type 2=0.06). There was no clear support for models
377 ran using the extended mtDNA-only dataset, which included the 16 colonies and all the
378 individual samples. Although Scenario 1.4 (West source, colonised East via South) received

379 relatively high support (posterior probability=0.73), error rates were high (type 1=0.39, type
380 2=0.32), indicating that the analysis was unable to differentiate between the scenarios.

381 **Discussion**

382 The combination of climate change and topographically originated environmental
383 heterogeneity played an important role in shaping the evolutionary history and current genetic
384 population structure of *M. escalerae* within the Iberian refugium, and it is likely to continue
385 shaping the future distribution and patterns of genetic diversity of this restricted range
386 endemic species.

387 **The biogeographic history of *Myotis escalerae***

388 It is not clear what event caused the divergence of *M. escalerae* from its Moroccan cryptic
389 sister species *M. spB* around 0.99 million years ago (Salicini *et al.* 2013). However, despite
390 this relatively recent speciation event we found strong support for divergence into distinct
391 clades. Quaternary climatic oscillations appear to have left a signature of geographic
392 population structure in *M. escalerae* which corresponds to patterns of deep lineage divergence
393 in other Iberian taxa whose lineages diverged before the Pleistocene (e.g. the *Vipera*
394 *latastei/monticola* group, Velo-Anton *et al.* 2012).

395 Based on the mtDNA dataset, *M. escalerae* across Iberia is divided into three main lineages,
396 the Western clade, which is restricted to the Atlantic climatic region in Portugal, the North-
397 Central-Eastern clade, and the Southern clade. Paleo-SDMs indicate that this split may be the
398 result of the disjunct distribution of suitable climatic conditions during the LGM when
399 suitable areas were restricted to isolated patches in the west, east, south, and near the Pyrenees
400 and southern France. Model projections and the strong association of the phylogenetic divide

401 with geography lend support to the suggestion that during the Pleistocene several
402 geographically separate refugia were present within the Iberian refugium (Gomez & Lunt
403 2007; Ferrero *et al.* 2011). The strong genetic differentiation of a large number of Iberian
404 species into a western (Atlantic) and eastern (Mediterranean) lineages is thought to reflect the
405 disjunct LGM distribution of the most favourable climatic conditions in the peninsula
406 (Schmitt 2007) and the harsher climate of the central Iberian plateau that separates them
407 (Gomez & Lunt 2007).

408 Unlike other bat species for whom Iberia was the principal glacial refugia (e.g. *Plecotus*
409 *austriacus*; Razgour *et al.* 2013), *M. escaleraei* is unique as it has never expanded its range
410 beyond the peninsula, even though it is found across the Pyrenees, and therefore Iberia for
411 this species may represent an area of endemism rather than refugium (Stewart *et al.* 2010).
412 Other Iberian endemics, like *Galemys pyrenaicus*, show similar patterns of divergence into
413 distinct evolutionary lineages, suggesting the existence of complex isolation mechanisms as
414 species experienced whole glacial processes of contraction and dispersal within the peninsula
415 (Igea *et al.* 2013).

416 ABC model-based inference confirms the presence of separate western and eastern refugia
417 during the LGM, and has identified the source populations of each geographical group as
418 colonies that experienced suitable climatic conditions during the LGM based on SDM
419 projections. Moreover, in line with SDM projections of climatic suitability during the LIG,
420 evolutionary history inference suggests that the Western group was the source population.
421 The concordance between the projected distribution of suitable climatic conditions during the
422 LGM and LIG based on SDMs and evolutionary history inference based on genetic data lends
423 support to the presence of niche conservatism in climatic tolerance in *M. escaleraei*. Niche

424 conservatism may limit the ability of species to adapt to novel environmental conditions
425 within the timeframe required to respond to climate changes, suggesting that instead species
426 will either shift their geographic ranges to track suitable climatic regimes or go extinct (Wiens
427 & Graham 2005). However, Pellissier et al. (2013) show that, at least for arctic-alpine plant
428 species, niche conservatism is more pronounced at cold than warm thermal limits because
429 biotic interactions (e.g. competition) play a more important role when conditions are less
430 severe and species are not at their physiological limits.

431 Yet, climate and topography alone do not determine a species' occurrence, as is evident from
432 the full SDM, in which habitat variables, and in particular the presence of coniferous
433 woodlands, was a strong determinant of occurrence probability. Predicted distribution of
434 forest tree species in Iberia during the LGM (Benito Garzón *et al.* 2007) and evidence from
435 pollen records (Gomez & Lunt 2006; Lopez de Heredia *et al.* 2007; Rodriguez-Sanchez *et al.*
436 2010) suggest that most of the studied colonies were located in areas where forests persisted
437 during the LGM. Therefore forest availability is not likely to have been a major limiting
438 factor for *M. escalerai* during colder periods. Although LGM forests were dominated by pines
439 (Rodriguez-Sanchez *et al.* 2010), the main woodland type where *M. escalerai* is currently
440 found based on the full SDM, south and south-western Iberia were less forested and
441 dominated by evergreen oaks (Benito Garzón *et al.* 2007). This may explain the ABC
442 inference that *M. escalerai* persisted during the LGM in Western and Eastern areas, while the
443 south was only colonised around the early-mid-Holocene when the predicted distribution of
444 pines extended to the south-west (Benito Garzón *et al.* 2007).

445 **Current patterns of genetic variability and future losses**

446 Population assignment and geographical separation was less clear at the microsatellite than
447 the mtDNA level. Only a slight signature of a geographical West and East divide was evident,
448 most colonies were assigned to more than one genetic population cluster and many
449 individuals showed some level of admixture. Moreover, colony assignment into geographical
450 groups did not always follow the same pattern as the mtDNA dataset. For example, based on
451 the mtDNA dataset, the north-western colony Ourense belongs to the North-Central-Eastern
452 lineage, despite being geographically close to one of the Western colonies, while the
453 microsatellite dataset groups Ourense with the Western colonies. This inconsistency in
454 population assignment may reflect the effect of recent (post-LGM) gene flow disguising older
455 population splits. Microsatellites with their higher evolutionary rates reflect recent or
456 contemporary genetic patterns, while mtDNA is more informative of events that occurred
457 during earlier periods of the species' history (Wan *et al.* 2004).

458 Alternatively, more limited population structure at the microsatellite level may be the result of
459 male-biased dispersal and female philopatry, a common pattern in bat species (Burland &
460 Worthington Wilmer 2001). Ruedi and Castella (2003) identified a similar pattern in *Myotis*
461 *myotis*, attributing the absence of population structure at the microsatellite level versus the
462 strong population structure and limited gene flow between colonies at the mtDNA level to the
463 estimated male bias in the proportion of dispersing individuals (>90%). These disparities
464 highlight the importance of combining bi-parentally inherited nuclear markers and maternally
465 inherited mtDNA markers with different evolutionary rates in phylogeographic studies.

466 Genetic diversity, based on both the mtDNA and microsatellite datasets, is highest in southern
467 colonies, despite their more recent evolutionary history based on the ABC inference.

468 Although this region contains several unique haplotypes and private alleles, high levels of
469 genetic diversity may also be due to this region acting as a ‘hybrid/contact zone’ between the
470 Western and Eastern refugia, in which genetic diversity was enriched by the admixture of
471 divergent lineages (Hewitt 2011). And indeed southern colonies include haplotypes that group
472 with both the Western and North-Central-Eastern clades. On the other hand, high levels of
473 inbreeding and reduced allelic diversity in the most north-eastern colony (Girona) and the
474 island colony (Illes Balears) may reflect their geographic isolation and limited recent gene
475 flow from other populations. In the north-eastern colony in particular, high coancestry values
476 likely reflect inbreeding in a small isolated population, rather than relatedness due to natal
477 philopatry and the presence of mothers and their pups, because this is the only location where
478 samples were collected from a swarming site and not a maternity colony. While bat summer
479 maternity colonies can include a high proportion of relatives due to strong female natal
480 philopatry, during the autumn, the closely related *Myotis nattereri* tends to migrate away from
481 summer roosts to swarming sites that serve large catchment areas of up to 60 km (Rivers *et al.*
482 2006).

483 Under future climate change projections, the relative occurrence probability of *M. escaleraei*
484 across most of Iberia is predicted to decrease substantially. Range losses are predicted to be
485 greatest in the south, placing the entire southern lineage in climatically unsuitable areas by
486 2070. Although low levels of population differentiation between Southern colonies and both
487 Western and North-Central-Eastern colonies indicate the presence of gene flow under current
488 conditions, range fragmentation is likely to increase in the future, resulting in colony
489 isolation. Increased isolation can limit future range shifts and lead to increased inbreeding and
490 loss of genetic diversity (Frankham 1995). Future climate change poses a particular threat to
491 *M. escaleraei* because it is restricted to the Iberian Peninsula where changes are predicted to be

492 particularly severe (EEA 2012). Other drivers of environmental change, and in particular
493 anthropogenic habitat loss, may hamper the ability of low dispersal and habitat specialist
494 species, like *M. escalerae*, to shift their ranges in response to climate changes (Warren *et al.*
495 2001).

496 Forests are predicted to show a time lag in their response to climate change at their trailing
497 edge. Increased temperatures and frequency of droughts are predicted to reduce seedling
498 recruitment and forest regeneration, but adult trees may be able persist in climatically
499 unsuitable areas due to their longevity and phenotypic plasticity (Jump *et al.* 2009). Because
500 forests provide cooler microclimates that can help buffer the effects of macroclimatic
501 warming (De Frenne *et al.* 2013), *M. escalerae* colonies may be able to persist in climatically
502 unsuitable areas in the short-term owing to their association with forests. Yet in the longer
503 term, modelling studies predict severe range contractions of mountain conifer, Mediterranean
504 and sub-Mediterranean forests in central and southern parts of the Iberian Peninsula (Benito
505 Garzón *et al.* 2008)

506 **What restricts an endemic species**

507 SDMs predict that suitable areas for *M. escalerae* are available outside the Iberian Peninsula,
508 in particular along the Mediterranean coast of France. Although extensive genetic sampling
509 has not yet taken place, both Salicini *et al.* (2013) and Puechmaille *et al.* (2012) genetically
510 identified all samples beyond the Eastern French Pyrenees as its congener *Myotis spA*.

511 Individual samples from around the Pyrenees, including the French Pyrenees, fell within the
512 North-Central-Eastern clade and mostly belonged to the common Eastern haplotype,
513 suggesting that this area was colonised from the Eastern refugia, rather than from a putative
514 'northern refugia' (Stewart & Lister 2001).

515 The range of *M. escalerai* is at least partly restricted by geographical barriers, the Gibraltar
516 Straits in the south and the Pyrenees mountain range in the north (Salicini *et al.* 2013), though
517 the Pyrenees themselves do not appear to form a barrier (Evin *et al.* 2009; Puechmaille *et al.*
518 2012). The Iberian Peninsula is home to several other restricted range endemic species, whose
519 limited dispersal abilities prevent them from crossing these geographical barriers, and as a
520 result their entire evolutionary history took place within Iberia (e.g. Igea *et al.* 2013).

521 Although flight offers bats greater vagility, the Pyrenees have formed a geographical barrier
522 for several bat species, restricting both post-glacial range re-colonisation from this refugium
523 (Rebelo *et al.* 2012; Dool *et al.* 2013) and current patterns of gene flow (Razgour *et al.* 2014).
524 Similarly, the Gibraltar Straits delimit the range of several bat species despite their relative
525 narrow breadth (Garcia-Mudarra *et al.* 2009).

526 However, because *M. escalerai* is found across the Pyrenees, including the French side of the
527 Eastern Pyrenees (Evin *et al.* 2009; Puechmaille *et al.* 2012), ecological rather than
528 geographical barriers may have played a more important role. Interspecific competition with
529 its cryptic congeners *M. spA* and *M. nattereri s.s.* that may occupy similar ecological niches
530 across the rest of Europe (Salicini *et al.* 2013) could have limited the spread of *M. escalerai*
531 beyond the Pyrenees. It is possible that a delay in northward population expansion post-LGM
532 due to the longer persistence of ice cover in the Pyrenees meant that advancing competing
533 congeners from the Italian and Balkan refugia restricted the space available for *M. escalerai*
534 north of the Pyrenees, as has been postulated for some Iberian forest tree lineages (Rodriguez-
535 Sanchez *et al.* 2010). This suggests that future range gains predicted around the north coast of
536 Iberia, where *M. escalerai* is sympatric with *M. spA*, and in western France, north of the
537 Pyrenees, where *M. nattereri s.s.* is present, may not help offset extensive range losses in the
538 south and centre of Iberia because competitive exclusion may limit northern population

539 expansion. However, the presence of some altitudinal segregation in sympatric localities (J.
540 Juste, *personal observations*) could indicate different ecological optima for each of these two
541 species, which allow them to coexist in areas of range overlap.

542 **Conclusions**

543 A concentration of high genetic diversity and deeply differentiated evolutionary lineages in
544 Iberia has been found in other European bat species with limited long-distance dispersal
545 abilities (Ibáñez *et al.* 2006; Dool *et al.* 2013; Razgour *et al.* 2013), highlighting the
546 evolutionary importance of this peninsula for European bats. Here we resolve the spatial
547 genetic history of a species for which Iberia is not only a glacial refugium but also its range
548 limit, and therefore its future survival prospects are closely tied to climatic processes
549 occurring within the peninsula. We show that past climatic oscillations resulted in the
550 divergence of *M. escalerai* into separate Western and North-Central-Eastern populations,
551 supporting the ‘refugia within refugia’ hypothesis. In accordance with other studies of Iberian
552 reptiles and mammals, our ABC model-based inference and paleo-SDMs indicates that the
553 Western population is the older, source population. Although contemporary gene flow may
554 mask historic lineage splits, a signature of geographical population structure is still
555 maintained. The role of ecological barriers in restricting *M. escalerai* to the Iberian Peninsula
556 even during inter-glacial periods when climatic conditions are suitable elsewhere, suggest that
557 this species may be unable to shift its range north of the Pyrenees in the future when most of
558 the peninsula is predicted to become climatically unsuitable.

559 *M. escalerai* is a recently confirmed species (Ibáñez *et al.* 2006), whose global conservation
560 status is yet to be assessed, though within Portugal it is listed as vulnerable (Ministério do
561 Ambiente e do Ordenamento do Território 2010). Our findings suggest that conservation

562 management for this species should increase landscape connectivity across Iberia in order to
563 facilitate north-western range shifts in response to future climate change, especially from the
564 southern lineage that is particularly threatened by future changes.

565 **Acknowledgements**

566 We are grateful for the invaluable support provided by M. Bertozzi, J.L. García-Mudarra and
567 J. Nogueras in the field and laboratory, as well as to all the people who helped with the
568 collection of samples: H. Rebelo, H. Santos, T. Castelló, O. de Paz, D. Garcia, J. Quetglas, X.
569 Puig, C. Flaquer, A. López-Baucells, G. Schreur, R. Hermida and F. Lamas. Logistical
570 support was provided by Laboratorio de Ecología Molecular, Estación Biológica de Doñana,
571 CSIC (LEM-EBD) and the ISPRA Conservation Genetics Laboratory staff, and in particular
572 A. Viglino. I. Salicini benefited from a JAE (Junta para la Ampliación de Estudios'
573 programme) pre-doctoral fellowship from the Consejo Superior de Investigaciones Cientificas
574 (CSIC). The study was funded by projects 200430E330 of the CSIC, SAF2006-12784-C02-
575 02 of the Spanish Ministry of Science and Education, PPNN181/2010 of the Spanish Ministry
576 of Environment, and with support of the Spanish Severo Ochoa Program (SEV-2012-0262).
577 O. Razgour was funded by the University of Stirling Impact Fellowship.

578 **References**

- 579 Alvarado-Serrano DF, Knowles LL (2014) Ecological niche models in phylogeographic
580 studies: applications, advances and precautions. *Molecular Ecology Resources*, **14**,
581 233–248.
- 582 Araújo MB, Nogues-Bravo D, Diniz-Filho JAF *et al.* (2008) Quaternary climate changes
583 explain diversity among reptiles and amphibians. *Ecography*, **31**, 8–15.
- 584 Avise JC (2000) *Phylogeography: The History and Formation of Species*. Harvard University
585 Press, Massachusetts, USA.

- 586 Benito Garzón M, Sanchez de Dios R, Sainz Ollero H (2007) Predictive modelling of tree
587 species distributions on the Iberian Peninsula during the Last Glacial Maximum and
588 Mid-Holocene. *Ecography*, **30**, 120–134.
- 589 Benito Garzón M, Sanchez de Dios R, Sainz Ollero H (2008) Effects of climate change on the
590 distribution of Iberian tree species. *Applied Vegetation Science*, **11**, 169–178.
- 591 Burland TM, Worthington Wilmer J (2001) Seeing in the dark: molecular approaches to the
592 study of bat populations. *Biology Reviews*, **76**, 389–409.
- 593 Castella V, Ruedi M (2000) Characterization of highly variable microsatellite loci in the bat
594 *Myotis myotis* (Chiroptera: Vespertilionidae). *Molecular Ecology*, **9**, 1000–1002.
- 595 Cornuet JM, Ravigné V, Estoup A (2010) Inference on population history and model
596 checking using DNA sequence and microsatellite data with the software DIYABC
597 (v1.0). *BMC Bioinformatics*, **11**, 401.
- 598 Cornuet J-M, Pudlo P, Veyssier J, Dehne-Garcia A, Gautier M, Leblois R, Marin J-M, Estoup
599 A (2014) DIYABC v2.0: a software to make Approximate Bayesian Computation
600 inferences about population history using Single Nucleotide Polymorphism, DNA
601 sequence and microsatellite data. *Bioinformatics*, **30**, 1187–1189.
- 602 Darriba D, Taboada GL, Doallo R, Posada D (2012) jModelTest 2: more models, new
603 heuristics and parallel computing. *Nature Methods*, **9**, 772.
- 604 De Frenne P, Rodriguez-Sanchez F, Coomes DA, *et al.* (2013) Microclimate moderates plant
605 population responses to macroclimate warming. *Proceedings of the National Academy
606 of Sciences of the USA*, **110**, 18561–18565.
- 607 Dool SE, Puechmaille SJ, Dietz C *et al.* (2013) Phylogeography and postglacial
608 recolonization of Europe by *Rhinolophus hipposideros*: evidence from multiple
609 genetic markers. *Molecular Ecology*, **22**, 4055–4070.
- 610 Earl DA, von Holdt BM (2012) STRUCTURE HARVESTER: a website and program for
611 visualizing STRUCTURE output and implementing the Evanno method. *Conservation
612 Genetics Resources*, **4**, 359–361.
- 613 EEA (2012) *Climate change, impacts and vulnerability in Europe 2012: an indicator-based
614 report*. EEA Report no. 12/2012. EEA, Copenhagen.
615 <http://www.eea.europa.eu/publications/climate-impacts-and-vulnerability-2012>
- 616 Evin A, Lecoq V, Durand M-O, Tillon L, Pons J-M (2009) A new species for the French bat
617 list: *Myotis escaleraei* (Chiroptera: Vespertilionidae). *Mammalia*, **73**, 142–144.
- 618 Ferrero ME, Blanco-Aguiar JA, Loughheed SC, Sanchez-Barbudo I, De Nova PJG,
619 Villafuerte R, Davila JA (2011) Phylogeography and genetic structure of the red-
620 legged partridge (*Alectoris rufa*): more evidence for refugia within the Iberian glacial
621 refugium. *Molecular Ecology*, **20**, 2628–2642.
- 622 Frankham R (1995) Effective population size / adult population size ratios in wildlife: a
623 review. *Genetical Research*, **66**, 95–107
- 624 García-Mudarra JL, Ibáñez C, Juste J (2009) The straits of Gibraltar: barrier or bridge to
625 Ibero-Moroccan bat diversity? *Biological Journal of the Linnean Society*, **96**, 434–
626 450.
- 627 Gomez A, Lunt DH (2007) Refugia within refugia: patterns of phylogeographic concordance
628 in the Iberian Peninsula. Ch. 5 in Weiss S, Ferrand N (Eds.). *Phylogeography of
629 Southern European Refugia: Evolutionary Perspectives on the Origins and
630 Conservation of European Biodiversity*. Springer, Dordrecht, the Netherlands, pp 155–
631 188.
- 632 Goudet J (1995) FSTAT (Version 1.2): A computer program to calculate F-statistics. *Journal
633 of Heredity*, **86**, 485–486.

- 634 Hampe A, Petit R (2005) Conserving biodiversity under climate change: the rear edge
635 matters. *Ecology Letters*, **8**, 461–467.
- 636 Hansen MC, Potapov PV, Moore R *et al.* (2013) High resolution global maps of 21st century
637 forest cover change. *Science*, **342**, 850–853.
- 638 Hewitt GM (2000) The genetic legacy of the Quaternary ice ages. *Nature*, **405**, 907–913.
- 639 Hewitt GM (2001) Speciation, hybrid zones and phylogeography – or seeing genes in space
640 and time. *Molecular Ecology*, **10**, 537–549.
- 641 Hewitt GM (2004) Genetic consequences of climatic oscillations in the Quaternary.
642 *Philosophical Transactions of the Royal Society of London B.*, **359**, 183–195.
- 643 Hickerson MJ, Carstens BC, Cavender-Bares J *et al.* (2010) Phylogeography’s past, present,
644 and future: 10 years after Avise, 2000. *Molecular Phylogenetics and Evolution*, **54**,
645 291–301.
- 646 Hofreiter M, Stewart JR (2009) Ecological change, range fluctuations and population
647 dynamics during the Pleistocene. *Current Biology*, **19**, R584–R594.
- 648 Hollingsworth E, Brahana V, Inlander E, Slay M (2008) Karst regions of the world (KROW):
649 global karst datasets and maps to advance the protection of karst species and habitats
650 worldwide. USGS Scientific Investigation Report 2008-5023.
651 <<http://pubs.usgs.gov/sir/2008/5023/06hollings.htm>>
- 652 Ibáñez C, García–Mudarra JL, Ruedi M, Stadelmann B, Juste J (2006) The Iberian
653 contribution to cryptic diversity in European bats. *Acta Chiropterologica*, **8**, 277–297.
- 654 Igea J, Aymerich P, Fernandez-Gonzalez A *et al.* (2013) Phylogeography and postglacial
655 expansion of the endangered semi-aquatic mammal *Galemys pyrenaicus*. *BMC*
656 *Evolutionary Biology*, **13**, 115.
- 657 IPCC (2013) Climate Change 2013: The Physical Science Basis. Working Group I
658 Contribution to the Fifth Assessment Report of the Intergovernmental Panel on
659 Climate Change (Eds. Stocker TF, Qin D, Plattner G-K *et al.*). Cambridge University
660 Press, Cambridge, UK and New York, USA.
- 661 Jombart T (2008) Adegnet: a R package for the multivariate analysis of genetic markers.
662 *Bioinformatics*, **24**, 1403–1405.
- 663 Jump AS, Matyas C, Peñuelas J (2009) The altitude-for-latitude disparity in the range
664 retractions of woody species. *Trends in Ecology and Evolution*, **24**, 694–701.
- 665 Kalinowski ST, Taper ML, Marshall TC (2007) Revising how the computer program
666 CERVUS accommodates genotyping error increases success in paternity assignment.
667 *Molecular Ecology*, **16**, 1099–1006.
- 668 Kerth G, Safi K, König B (2002) Mean colony relatedness is a poor predictor of colony
669 structure and female philopatry in the communally breeding Bechstein’s bat (*Myotis*
670 *bechsteinii*). *Behavioural Ecology and Sociobiology*, **52**, 203–210.
- 671 Librado P, Rozas J (2009) DnaSP v5: A software for comprehensive analysis of DNA
672 polymorphism data. *Bioinformatics*, **25**, 1451–1452.
- 673 Liu C, White M, Newell G (2013) Selecting thresholds for the prediction of species
674 occurrence with presence-only data. *Journal of Biogeography*, **40**, 778–789.
- 675 Lopez de Heredia U, Carrion JS, Jimenez P, Collada C, Gil L (2007) Molecular and
676 palaeoecological evidence for multiple glacial refugia for evergreen oaks on the
677 Iberian Peninsula. *Journal of Biogeography*, **34**, 1505–1517.
- 678 Merow C, Smith MJ, Silander JA (2013) A practical guide to MaxEnt for modeling species’
679 distributions: what it does, and why inputs and settings matter. *Ecography*, **36**, 1058–
680 1069.

- 681 Ministério do Ambiente e do Ordenamento do Território (2010) Agreement on the
682 Conservation of Populations of European Bats. Report on implementation of the
683 Agreement in Portugal 2010/6/MoP
- 684 Peakall R, Smouse PE (2006) GENALEX 6: genetic analysis in Excel. Population genetic
685 software for teaching and research. *Molecular Ecology Notes*, **6**, 288–295.
- 686 Pellissier L, Bråthen KA, Vittoz P *et al.* (2013) Thermal niches are more conserved at cold
687 than warm limits in arctic-alpine plant species. *Global Ecology and Biogeography*, **22**,
688 933–941.
- 689 Phillips SJ, Anderson RP, Schapire RE (2006) Maximum entropy modelling of species
690 geographic distributions. *Ecological Modelling*, **190**, 231–259.
- 691 Pritchard JK, Stephens M, Donnelly P (2000) Inference of population structure using
692 multilocus genotype data. *Genetics*, **155**, 945–959.
- 693 Puechmaille SJ, Allegrini B, Boston ESM *et al.* (2012) Genetic analyses reveal further cryptic
694 lineages within the *Myotis nattereri* species complex. *Mammalian Biology*, **77**, 224–
695 228.
- 696 Raes N, ter Steege H (2007) A null-model for significance testing of presence-only species
697 distribution models. *Ecography*, **30**, 727–736.
- 698 Raymond M, Rousset F (1995) GENEPOP (v1.2): population genetics software for exact tests
699 and ecumenicism. *Journal of Heredity*, **86**, 248–249.
- 700 Razgour O, Juste J, Ibáñez C *et al.* (2013) The shaping of genetic variation in edge-of-range
701 populations under past and future climate change. *Ecology Letters*, **16**, 1258–1266.
- 702 Razgour O, Rebelo H, Puechmaille SJ *et al.* (2014) Scale-dependent effects of landscape
703 variables on gene flow and population structure in bats. *Diversity and Distributions*,
704 **20**, 1173–1185.
- 705 Rebelo H, Froufe E, Brito JC *et al.* (2012) Postglacial colonization of Europe by the
706 barbastelle bat: agreement between molecular data and past predictive modelling.
707 *Molecular Ecology*, **21**, 2761–2774.
- 708 Rivers NM, Butlin RK, Altringham JD (2006) Autumn swarming behaviour of Natterer's bats
709 in the UK: population size, catchment area and dispersal. *Biological Conservation*,
710 **127**, 215–226.
- 711 Rodriguez-Ramilo ST, Wang J (2012) The effect of close relatives on unsupervised Bayesian
712 clustering algorithms in population genetic structure analysis. *Molecular Ecology*
713 *Resources*, **12**, 873–884.
- 714 Rodriguez-Sanchez F, Hampe A, Jordano P, Arroyo J (2010) Past tree range dynamics in the
715 Iberian Peninsula inferred through phylogeography and palaeodistribution modelling:
716 A review. *Review of Palaeobotany and Palynology*, **162**, 507–521.
- 717 Ronquist F, Huelsenbeck JP (2003) MrBayes 3: Bayesian phylogenetic inference under mixed
718 models. *Bioinformatics*, **19**, 1572–1574.
- 719 Rosenberg NA (2004) DISTRUCT: a program for the graphical display of population
720 structure. *Molecular Ecology Notes*, **4**, 137–138.
- 721 Rousset F (2008) GENEPOP'007: a complete re-implementation of the GENEPOP software
722 for Windows and Linux. *Molecular Ecology Resources*, **8**, 103–106.
- 723 Ruedi M, Castella V (2003) Genetic consequences of the ice ages on nurseries of the bat
724 *Myotis myotis*: a mitochondrial and nuclear survey. *Molecular Ecology*, **12**, 1527–
725 1540.
- 726 Salicini I, Ibáñez C, Juste J (2011) Multilocus phylogeny and species delimitation within the
727 Natterer's bat species complex in the Western Palearctic. *Molecular Phylogenetics and*
728 *Evolution*, **61**, 888–898.

- 729 Salicini I, Ibáñez C, Juste J (2013) Deep differentiation between and within Mediterranean
730 glacial refugia in a flying mammal, the *Myotis nattereri* bat complex. *Journal of*
731 *Biogeography*, **40**, 1182–1193.
- 732 Schmitt T (2007) Molecular biogeography of Europe: Pleistocene cycles and postglacial
733 trends. *Frontiers in Zoology*, **4**, 11.
- 734 Stewart JR, Lister AM (2001) Cryptic northern refugia and the origins of the modern biota.
735 *Trends in Ecology and Evolution*, **16**, 608–613.
- 736 Stewart JR, Lister AM, Barnes I, Dalen L (2010) Refugia revisited: individualistic responses
737 of species in space and time. *Proceedings of the Royal Society of London B.*, **277**,
738 661–671.
- 739 Van Oosterhout C, Hutchinson WF, Wills DPM, Shipley P (2004) MICRO-CHECKER:
740 software for identifying and correcting genotyping errors in microsatellite data.
741 *Molecular Ecology Notes*, **4**, 535–538.
- 742 VanDerWal J, Shoo LP, Graham C, Williams SE (2009) Selecting pseudo-absence data for
743 presence-only distribution modeling: How far should you stray from what you know?
744 *Ecological Modelling*, **220**, 589–594.
- 745 Velo-Anton G, Godinho R, Harris DJ *et al.* (2012) Deep evolutionary lineages in a Western
746 Mediterranean snake (*Vipera latastei/monticola* group) and high genetic structuring in
747 Southern Iberian populations. *Molecular Phylogenetics and Evolution*, **65**, 965–973.
- 748 Wan Q-H, Wu H, Fujihara T, Fang S-G (2004) Which genetic marker for which conservation
749 genetics issue? *Electrophoresis*, **25**, 2165–2176.
- 750 Wang J (2007) Triadic IBD coefficients and applications to estimating pairwise relatedness.
751 *Genetic Resources*, **89**, 135–153.
- 752 Wang J (2011) COANCESTRY: A program for simulating, estimating and analysing
753 relatedness and inbreeding coefficients. *Molecular Ecology Resources*, **11**, 141–145.
- 754 Warren DL, Glor RE, Turelli M (2010) ENMTools: a toolbox for comparative studies of
755 environmental niche models. *Ecography*, **33**, 607–611.
- 756 Warren MS, Hill JK, Thomas JA *et al.* (2001) Rapid responses of British butterflies to
757 opposing forces of climate and habitat change. *Nature*, **414**, 65–69.
- 758 Wiens JJ, Graham CH (2005) Niche Conservatism: Integrating Evolution, Ecology, and
759 Conservation Biology. *Annual Review of Ecology, Evolution, and Systematics*, **36**,
760 519–539.
- 761 Xia X, Xie Z (2001) DAMBE: Data analysis in molecular biology and evolution. *Journal of*
762 *Heredity*, **92**, 371–373.

763 **Data Accessibility**

- 764 - DNA sequences will be submitted to Genbank upon manuscript acceptance and accessions
765 numbers will be provided.
- 766 - MaxEnt output files will be made available on Dryad
- 767 - Sampling locations and microsatellite genotypes will be made available on Dryad

768 **Author Contribution**

769 CI, IS and JJ designed the study, collected or organised the sample collection, generated the
770 molecular data and contributed to the manuscript. ER helped with obtaining the microsatellite
771 dataset and information at ISPRA Conservation Genetics Laboratory and contributed to the
772 manuscript. OR wrote the manuscript and performed the genetic analysis (mtDNA and
773 microsatellite), species distribution modelling and ABC evolutionary history analysis.

774 **Figure Captions**

775 **Figure 1** – *Myotis escalerai* population structure based on the mtDNA (Cytochrome b)
776 dataset (colonies and individual samples, N=359). A) Map of the location of the colonies
777 (larger circles and names) and individual samples included in the study. B) Bayesian
778 phylogenetic tree showing posterior probability values >0.8. Haplotypes are named and
779 colour-coded based on their respective sampling locations. C) Median-joining haplotype
780 network, colour-coded based on location of origin. Diagonal stripes represent individual
781 samples from the same region as a colony of the same colour. Circle sizes correspond to
782 number of samples. Numbers indicate haplotypes separated by >1 mutation.

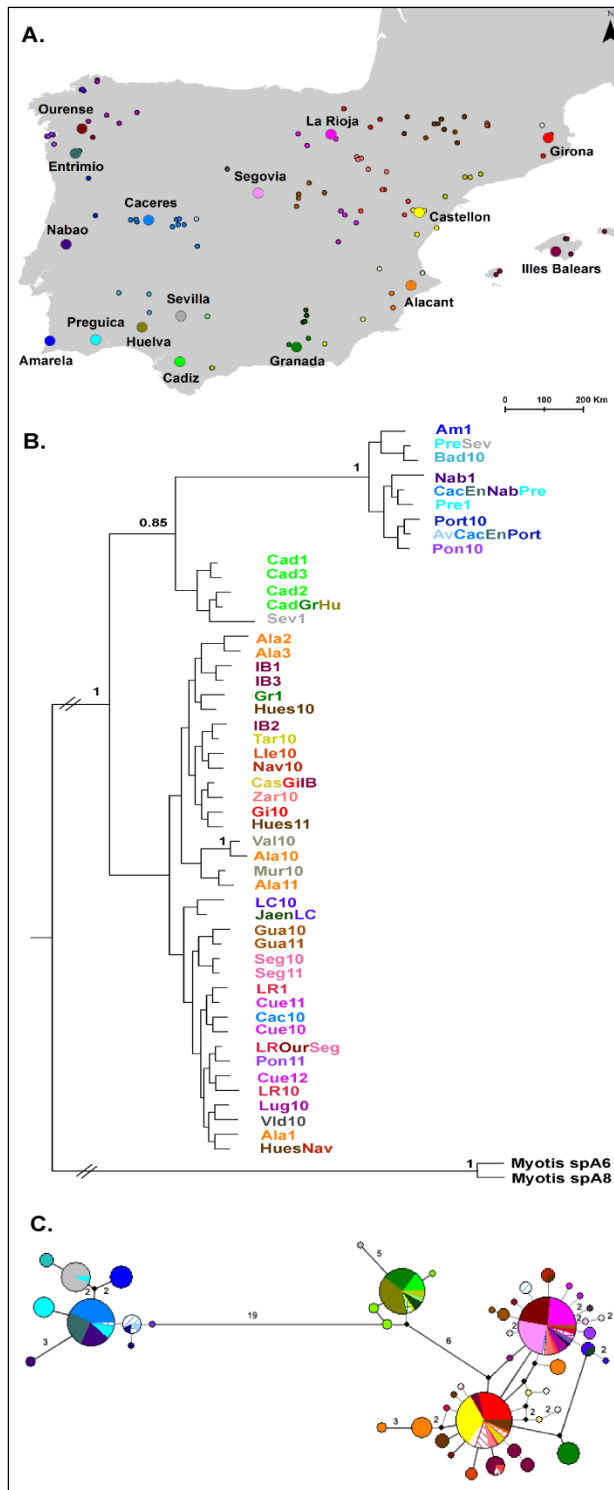
783 **Figure 2** – *Myotis escalerai* population structure based on the microsatellite dataset. A)
784 STRUCTURE analysis including all samples (K=4); and B) STRUCTURE analysis after
785 close relatives (TrioML>0.5) were removed (K=3), showing cluster membership plots and
786 frequency of each cluster in the studied colonies.

787 **Figure 3** – Species distribution models for *Myotis escalerai* across temporal scales: A-B)
788 present climate model, C-D) Last Glacial Maximum (LGM ~21,000 ybp), and E-F) future
789 (2070, +8.5rcp scenario). Models are presented as a scale of relative occurrence probability
790 from low in yellow to high in dark blue (A,C,E), or as binary maps of potentially suitable
791 areas in black (B,D,F). White circle denote the location of the studied colonies.

792 **Figure 4** – Results of the Approximate Bayesian Computation analysis of the evolutionary
793 history of *Myotis escalerai*, showing the selected scenarios for A) the full model, and B) the
794 Western and Eastern Group analyses. White circles denote the location of colonies. Arrows
795 represent the direction of colonisation from the source population, with median estimated
796 divergence dates.

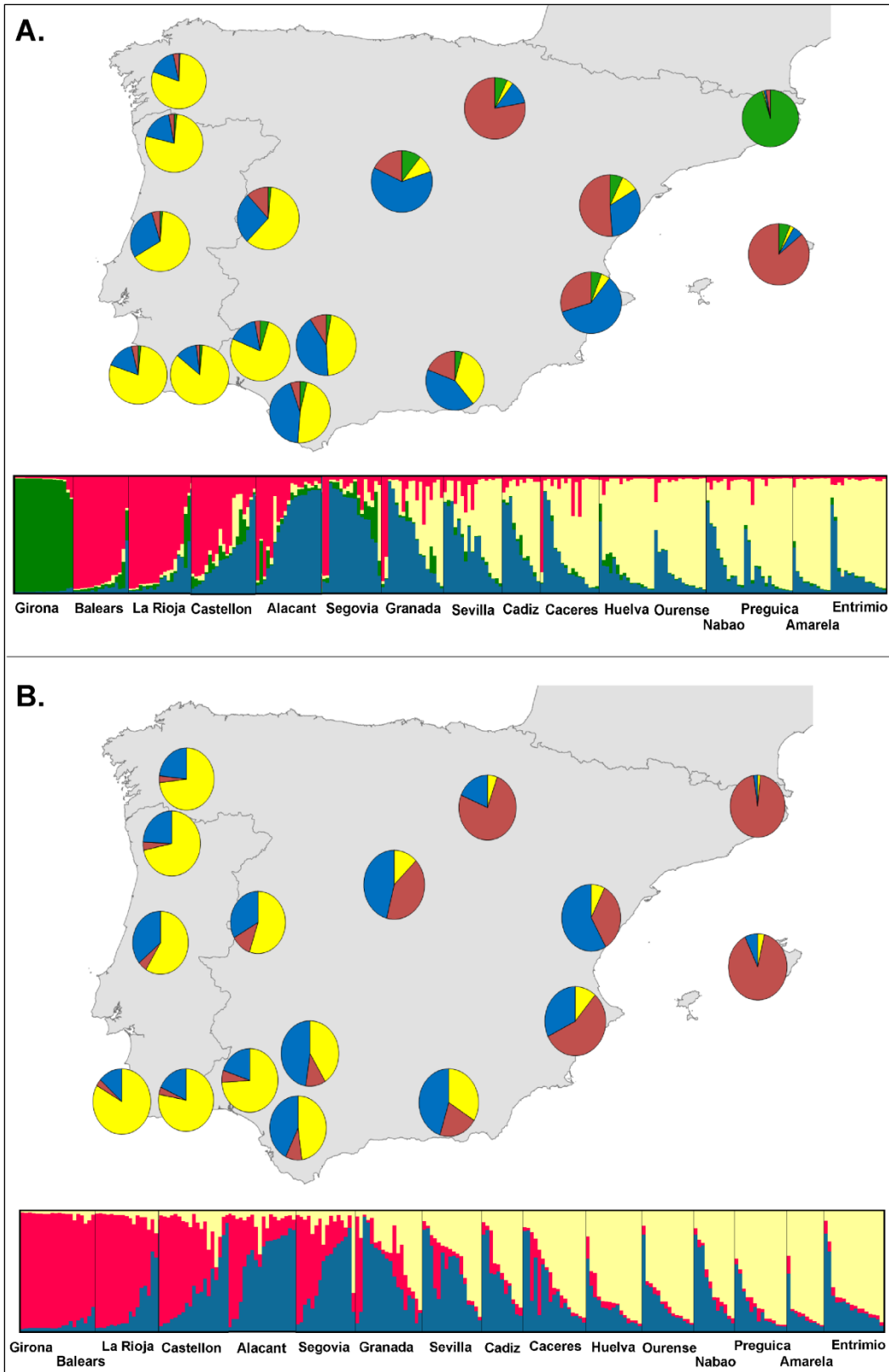
797 **Table 1** – Genetic diversity of *Myotis escalerai* colonies based the microsatellite (first six columns) and the *Cyt b* mtDNA (last four columns)
 798 datasets, with sample sizes presented in brackets. Mean allelic richness and gene diversity (\pm standard deviation) were adjusted based on sample
 799 size.

	Mean number of alleles	Shannon Index	Gene diversity	Allelic richness	Number of private alleles	Heterozygosity (He)	Number of haplotypes	Number of polymorphic sites	Haplotypic diversity	Nucleotide diversity (Pi)
Alacant (19)	7.44 \pm 1.0	1.593	0.76 \pm 0.1	6.0 \pm 2.2	0	0.739	3	8	0.608	0.0044
Amarela (11)	5.00 \pm 0.5	1.261	0.67 \pm 0.1	4.9 \pm 1.5	0	0.636	1	0	0	0
Cáceres (17)	7.33 \pm 1.1	1.609	0.75 \pm 0.2	6.3 \pm 2.6	3	0.728	1	0	0	0
Cádiz (11)	6.33 \pm 0.7	1.579	0.77 \pm 0.2	6.2 \pm 2.1	0	0.735	4	3	0.691	0.0014
Castellón (19)	7.22 \pm 1.0	1.586	0.74 \pm 0.2	6.1 \pm 2.3	0	0.719	1	0	0	0
Entrimio (16)	6.33 \pm 0.7	1.433	0.69 \pm 0.2	5.6 \pm 1.8	0	0.672	1	0	0	0
Girona (17)	3.44 \pm 0.7	0.792	0.44 \pm 0.3	3.1 \pm 1.6	0	0.431	1	0	0	0
Granada (18)	8.11 \pm 1.2	1.711	0.77 \pm 0.2	6.8 \pm 2.9	4	0.748	2	10	0.526	0.0070
Huelva (16)	6.00 \pm 0.7	1.440	0.70 \pm 0.2	5.4 \pm 2.0	0	0.681	1	0	0	0
I. Balears (16)	5.44 \pm 0.9	1.192	0.60 \pm 0.2	4.7 \pm 2.2	2	0.581	4	3	0.792	0.0019
La Rioja (18)	6.00 \pm 0.9	1.396	0.70 \pm 0.2	5.2 \pm 2.0	1	0.681	2	1	0.118	0.0002
Nabão (11)	5.78 \pm 0.7	1.474	0.74 \pm 0.2	5.6 \pm 2.0	0	0.702	2	3	0.327	0.0013
Ourense (15)	6.22 \pm 0.9	1.433	0.69 \pm 0.2	5.6 \pm 2.4	0	0.666	1	0	0	0
Preguiça (14)	5.67 \pm 0.6	1.305	0.65 \pm 0.2	5.2 \pm 1.5	0	0.622	3	4	0.538	0.0012
Segovia (17)	7.44 \pm 1.1	1.568	0.72 \pm 0.2	6.3 \pm 2.6	0	0.700	1	0	0	0
Sevilla (17)	7.56 \pm 1.0	1.600	0.75 \pm 0.1	6.3 \pm 2.2	0	0.728	2	25	0.111	0.0037



801
802
803
804
805
806
807
808
809

Figure 1 – *Myotis escalerai* population structure based on the mtDNA (Cytochrome b) dataset (colonies and individual samples, N=359). A) Map of the location of the colonies (larger circles and names) and individual samples included in the study. B) Bayesian phylogenetic tree showing posterior probability values >0.8. Haplotypes are named and colour-coded based on their respective sampling locations. C) Median-joining haplotype network, colour-coded based on location of origin. Diagonal stripes represent individual samples from the same region as a colony of the same colour. Circle sizes correspond to number of samples. Numbers indicate haplotypes separated by >1 mutation.



810

811

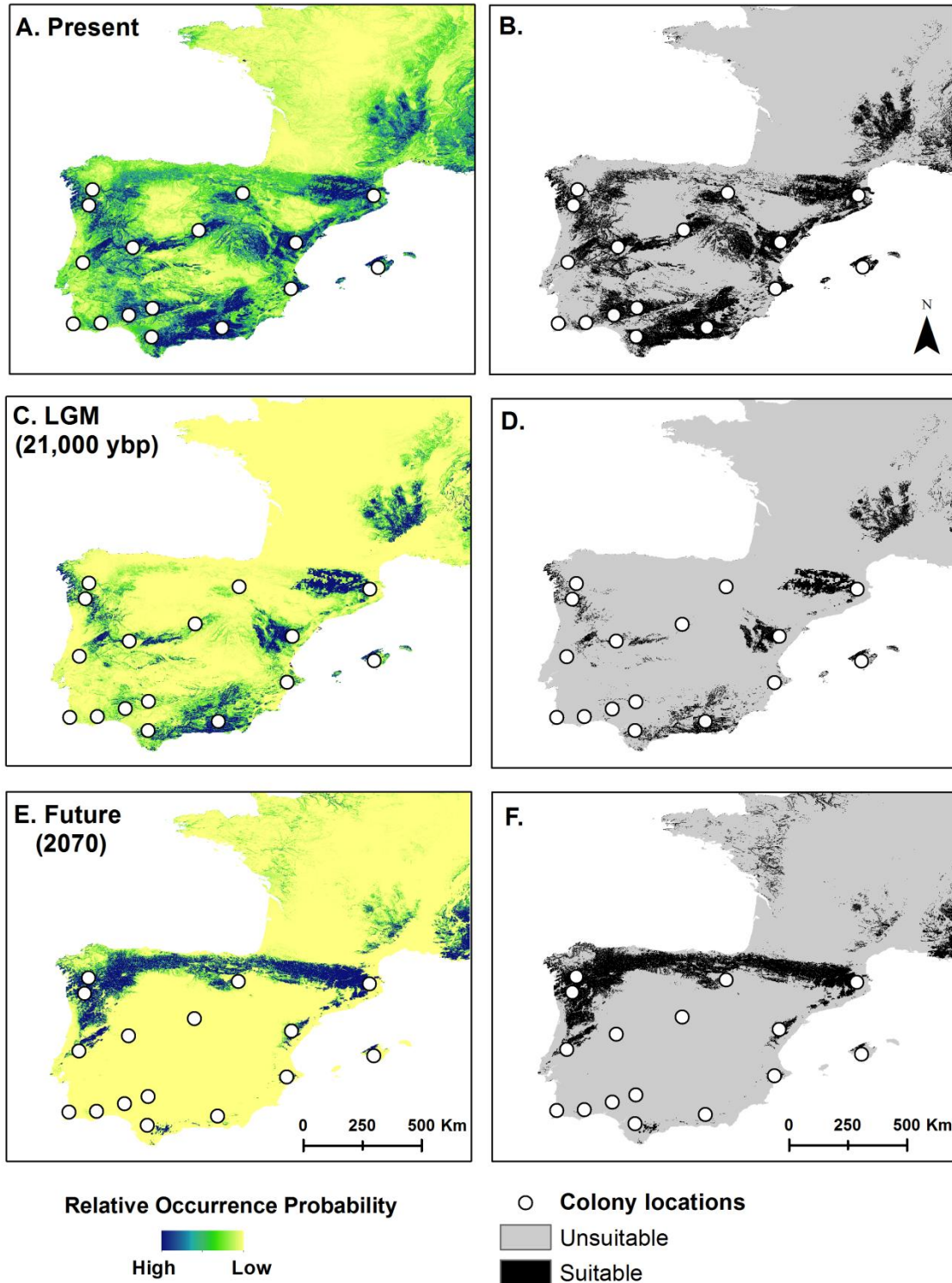
812

813

814

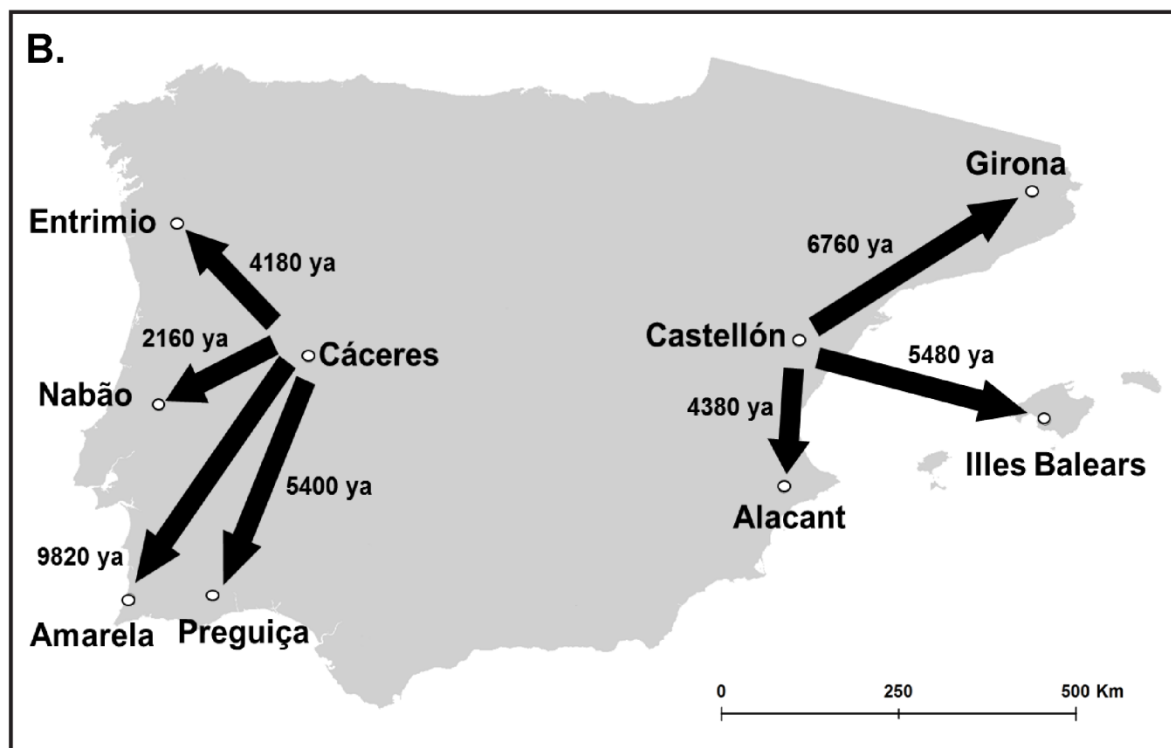
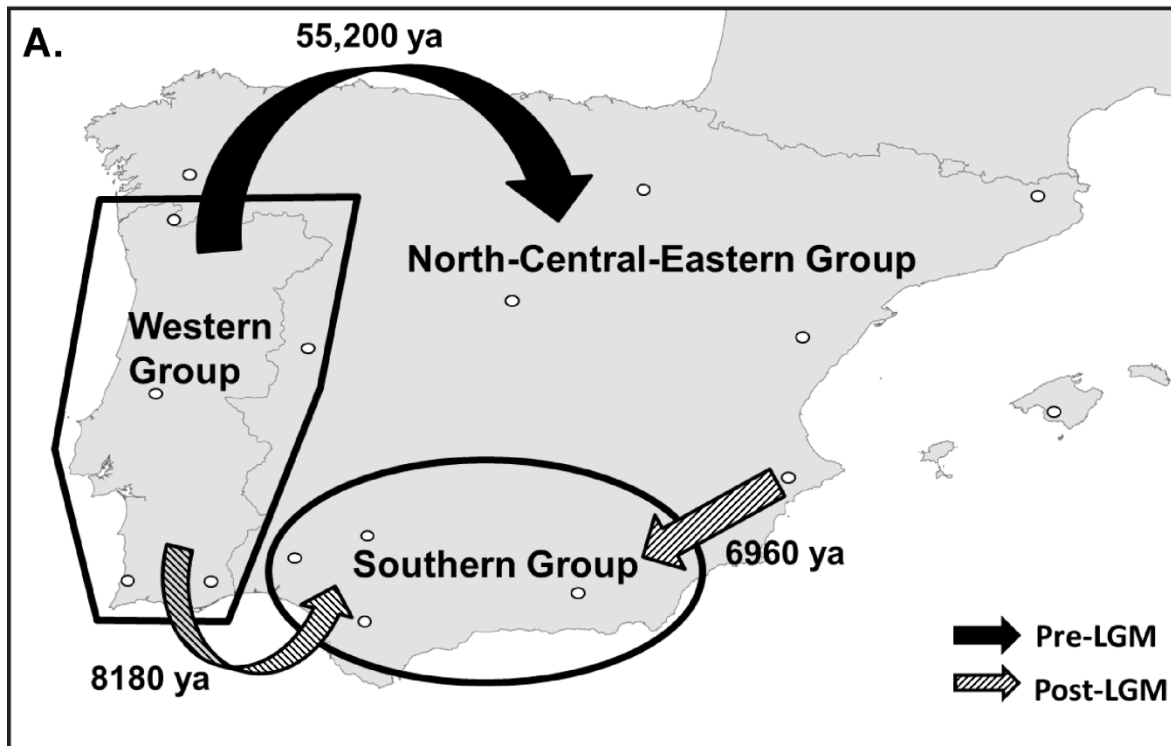
815

Figure 2 – *Myotis escalerai* population structure based on the microsatellite dataset. A) STRUCTURE analysis including all samples (K=4); and B) STRUCTURE analysis after close relatives (TriomL>0.5) were removed (K=3), showing cluster membership plots and frequency of each cluster in the studied colonies.



816

817 **Figure 3** – Species distribution models for *Myotis escaleraei* across temporal scales: A-B)
 818 present climate model, C-D) Last Glacial Maximum (LGM ~21,000 ybp), and E-F) future
 819 (2070, +8.5rcp scenario). Models are presented as a scale of relative occurrence probability
 820 from low in yellow to high in dark blue (A,C,E), or as binary maps of potentially suitable
 821 areas in black (B,D,F). White circle denote the location of the studied colonies.



822

823 **Figure 4** – Results of the Approximate Bayesian Computation analysis of the evolutionary
 824 history of *Myotis escalerai*, showing the selected scenarios for A) the full model, and B) the
 825 Western and Eastern Group analyses. White circles denote the location of colonies. Arrows
 826 represent the direction of colonisation from the source population, with median estimated
 827 divergence dates.